

Large- N_c gauge theory and chiral random matrix theory

Masanori HANADA^{1a}, Jong-Wan Lee^{2a} and Norikazu YAMADA^{3ab}

^a *KEK Theory Center*

High Energy Accelerator Research Organization (KEK)

Tsukuba 305-0801, Japan

^b *Department of Particle and Nuclear Physics*

Graduate University for Advanced Studies (SOKENDAI)

Tsukuba, Ibaraki 305-0801, Japan

abstract

We discuss how the $1/N_c$ expansion and the chiral random matrix theory (χ RMT) can be used in the study of large- N_c gauge theories. We first clarify the parameter region in which each of these two approaches is valid: while the fermion mass m is fixed in the standard large- N_c arguments ('t Hooft large- N_c limit), m must be scaled appropriately with a certain negative power of N_c in order for the gauge theories to be described by the χ RMT. Then, although these two limits are not compatible in general, we show that the breakdown of chiral symmetry can be detected by combining the large- N_c argument and the χ RMT with some cares. As a concrete example, we numerically study the four dimensional $SU(N_c)$ gauge theory with $N_f = 2$ heavy adjoint fermions, introduced as the center symmetry preserver keeping the infrared physics intact, on a 2^4 lattice. By looking at the low-lying eigenvalues of the Dirac operator for a massless probe fermion in the adjoint representation, we find that the chiral symmetry is indeed broken with the expected breaking pattern. This result reproduces a well-known fact that the chiral symmetry is spontaneously broken in the pure $SU(N_c)$ gauge theory in the large- N_c and the large-volume limit, and therefore supports the validity of the combined approach. We also provide the interpretation of the gap and unexpected N_c -scaling, both of which are observed in the Dirac spectrum.

¹ E-mail address : hanada@post.kek.jp

² E-mail address : jongwan@post.kek.jp

³ E-mail address : norikazu.yamada@kek.jp

1 Introduction

From a field theoretical point of view, strongly coupled gauge theories such as quantum chromodynamics (QCD) are of great interest as they have a number of nontrivial phenomena in themselves. Because it is difficult to study those theories analytically, effective theory approaches and the large- N_c limit are often considered. For example, if one considers the low-energy limit of QCD (and also theories with spontaneous chiral symmetry breaking ($S\chi SB$)), the form of the low energy effective theory is tightly constrained by the symmetries so that one obtains the chiral Lagrangian. If we further go to the ϵ -regime, where the length of the box containing the system is much smaller than the pion Compton length, all such theories fall into one of three *universality classes*, which are exactly described by the chiral random matrix theory (χRMT). In Ref. [1] this property was used to demonstrate $S\chi SB$ from the first principles by confirming that the spectrum of the Dirac operator calculated on the lattice agrees with the χRMT prediction. Another example is the 't Hooft large- N_c limit [2]. In particular, the large- N_c volume independence (the so-called Eguchi-Kawai (EK) volume independence) [3] and the orbifold equivalence [4, 5] have recently received large attention in the context of the lattice Monte-Carlo simulation (see e.g. [6, 7, 8]).

Given remarkable successes of these two approaches, it is natural to consider how they can be combined to study various QCD-like theories. Once the combined approach has been established, it has several interesting applications. One of them is the search for the conformal window or the walking technicolor model (WTM), where the approach is used to see whether chiral symmetry is broken or not. A candidate of the minimal WTM is the $SU(2)$ gauge theory with two-flavors of fermions in the adjoint representation [9, 10]. So far, numerical results from (large-volume) lattice simulations indicate that this theory is inside the conformal window [11]. This situation may change when the number of colors increases from two. Then, the study of the large- N_c limit provides additional information useful to understand the phase diagram of the conformal window depicted in Ref. [12].

In this paper, we discuss how to utilize the χRMT and the large- N_c equivalence to study the large- N_c gauge theories, and provide the theoretical argument for the detection of $S\chi SB$ ⁴. It turns out that some cares are required because the valid parameter regions for these two techniques are different in general: in the χRMT limit (see Sec. 4 for the definition), the 't Hooft large- N_c expansion fails due to the non-trivial N_c -dependence of the expansion coefficients. Therefore, we cannot use the EK volume equivalence to relate the small-volume with the large-volume lattice theory in the χRMT limit. However, we argue that the chiral properties of the large-volume theory can still be studied from the small-lattice model with finite N_c by using the analytic continuation provided unbroken center symmetry.

Bearing the above motivation in mind, as a first step, we study pure $SU(N_c)$ gauge theories on a 2^4 lattice, aiming at taking the large- N_c limit. The goal is to find how we should extract physics in the large-volume limit from small lattice simulations. We call our theory on a 2^4 lattice as the 2^4 -lattice model to avoid a possible confusion with the EK model for which the 't Hooft limit is usually assumed. Following the argument by Eguchi and Kawai in the 't Hooft limit, we let our lattice theory keep the center symmetry by introducing two-flavors of heavy adjoint fermions

⁴In Ref. [6] and [13, 14], the authors already used the χRMT techniques for numerical studies of chiral symmetry breaking of $SU(N_c)$ gauge theories in the quenched limit and the theories with adjoint fermions, respectively. However, there is a subtlety (the difference of the limiting procedures explained in Sec. 4), which makes the conclusion ambiguous [14]. In this paper we clarify this point in order to fully justify the method.

⁵. But notice that the theory we deal with is essentially the pure $SU(N_c)$ gauge theory since they do not play any role in the low-energy dynamics. On the gauge configurations obtained, we calculate the low-lying spectrum of the Dirac operator in the adjoint representation and compare with the χ RMT prediction; an agreement between them should provide the evidence for $S\chi$ SB or equivalently non-zero chiral condensate in the 't Hooft limit. Using the EK volume equivalence, therefore, we conclude that chiral symmetry of pure $SU(N_c)$ gauge theory is indeed broken. While the agreement of the Dirac spectrum is confirmed as expected, the N_c -scaling of the spectrum turns out to be different from the one expected from the usual 't Hooft large- N_c counting. To be specific, we found that the eigenvalues scale as $1/N_c$ rather than $1/N_c^2$ at a reasonably weak coupling. We will present a possible explanation for this phenomenon in Sec. 5, which does not override the occurrence of $S\chi$ SB.

This paper is organized as follows. In Sec. 2, we review the 't Hooft large- N_c limit and its properties, especially the EK volume equivalence and the orbifold equivalence. In Sec. 3 we review the χ RMT - the definition and the relationship with the ϵ -regime of QCD-like theories with $S\chi$ SB. In Sec. 4 we discuss the difference of the χ RMT limit and the 't Hooft limit, in which we can use the χ RMT technique and the EK volume equivalence, respectively. Having this difference in mind, we explain how the χ RMT, combined with numerical simulations on a small lattice, can be used to study $S\chi$ SB of the large- N_c gauge theories. In Sec. 5 we present the numerical results of the 2^4 -lattice model; we first confirm that the center symmetry is unbroken in the presence of two-flavors of heavy adjoint fermions, and then proceed to the analysis of the Dirac spectrum including comparisons with the χ RMT prediction and determination of the N_c -scaling.

2 The 't Hooft large- N_c limit

Let us first consider the $SU(N_c)$ pure Yang-Mills theory,

$$S_{YM} = \frac{1}{4g_{YM}^2} \int d^4x \text{Tr} F_{\mu\nu}^2. \quad (1)$$

The 't Hooft large- N_c limit [2] is the large- N_c limit in which the 't Hooft coupling constant $\lambda = g_{YM}^2 N_c$ and the space-time V are fixed. ⁶ The energy scale under consideration (e.g. distance between operators, the size of the Wilson loop) is also fixed. In this limit the $1/N_c$ expansion has a natural topological structure,

$$\langle \hat{O} \rangle = \sum_{g=0}^{\infty} c_g(\lambda, V) N_c^{-2g}, \quad (2)$$

where \hat{O} is a properly normalized single trace operator. In the perturbation theory, contribution of order N_c^{-2g} comes from the genus- g nonplanar diagrams, i.e. the Feynman diagrams which can be drawn on the two-dimensional surface with g handles (Fig. 1). The connected correlation functions of more than one operators have the same structure. Therefore the $1/N_c$ -expansion

⁵Although we added two heavy adjoint fermions, one heavy adjoint fermion is good enough to keep the center symmetry [7, 13]

⁶More precisely, we take the coupling at some energy scale to be fixed. For example, in the case of the lattice regularization, we can take the bare lattice 't Hooft coupling to be the same. Then the beta function depends only on λ at large- N_c , and hence λ remains N_c -independent at any energy scale up to a $1/N_c$ -correction.

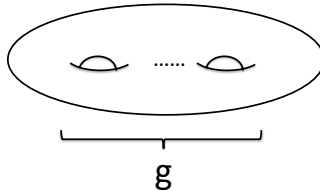


Figure 1: Two-dimensional surface of genus g .

is the same as the genus expansion. In the string theory, a genus- g surface corresponds to the string world-sheet with g closed string loops. Actually the Feynman diagrams can naturally be regarded as dynamical triangulations of the two-dimensional surfaces, and $1/N_c^2$ can be identified with the string coupling constant. In Maldacena's gauge/gravity duality conjecture [15], certain gauge theories are explicitly related to string theories. In the large- N_c limit, only the genus zero diagrams (planar diagrams) survive, or in the string terminology, the quantum string effect is suppressed at large- N_c .

Next let us consider QCD with N_f fundamental fermions. The fermionic part of the action is given by

$$S_{fermion} = \sum_{f=1}^{N_f} \int d^4x \bar{\psi}_f^{fund.} (\gamma^\mu D_\mu + m_f) \psi_f^{fund.}. \quad (3)$$

In the 't Hooft limit, in addition to the 't Hooft coupling and the space-time volume, the fermion mass m_f must also be fixed. Because the fermions have $O(N_f N_c)$ degrees of freedom while the gluons have $O(N_c^2)$, every time we replace the gluon loop with the fermion loop we obtain the factor N_f/N_c . Hence the $1/N_c$ -expansion becomes

$$\langle \hat{O} \rangle = \sum_{g,b=0}^{\infty} c_{g,b}(\lambda, V, m_f) N_c^{-2g} \cdot (N_f/N_c)^b, \quad (4)$$

where b is the number of fermion loops. Therefore, when N_f is fixed, diagrams with fermion loops are suppressed. (They are not suppressed if one considers the adjoint fermion instead.) In the 't Hooft large- N_c limit, the parameters λ , V and m_f are fixed, because otherwise a nontrivial N_c -dependence can appear through the coefficient $c_{g,b}(\lambda, V, m_f)$. For example, in QCD, if m_f decreases with N_c , N_c -dependent infrared divergence appears because the pion becomes lighter and the standard $1/N_c$ -counting in the 't Hooft limit can be destroyed completely.

In the 't Hooft large- N_c limit, various nice properties hold. Below we introduce the EK equivalence and the orbifold equivalence.

2.1 The large- N_c equivalences in the 't Hooft limit

2.1.1 The Eguchi-Kawai equivalence

Let us consider Wilson's lattice gauge theory on the L^4 periodic lattice,

$$S_W = 2N_c^2 b \sum_{\mathbf{n}} \sum_{\mu < \nu} \left(1 - \frac{1}{N_c} \text{ReTr} P_{\mu\nu}(\mathbf{n}) \right), \quad (5)$$

where μ, ν run from 1 to 4, $b = 1/\lambda = 1/(g_{YM}^2 N_c)$, \mathbf{n} runs through the L^4 lattice, and the plaquette $P_{\mu\nu}$ is given by

$$P_{\mu\nu}(\mathbf{n}) = U_{\mathbf{n},\mu} U_{\mathbf{n}+\mu,\nu} U_{\mathbf{n}+\nu,\mu}^\dagger U_{\mathbf{n},\nu}^\dagger. \quad (6)$$

The unitary link variables $U_{\mathbf{n},\mu}$ are related to the Hermitian gauge field A_μ by $U_{\mathbf{n},\mu} = e^{iaA_\mu(\mathbf{n})}$, where a is the lattice spacing. The nature of the theory is characterized by the expectation values of the Wilson loops

$$W(C) = \text{Tr} (U_{\mathbf{n},\mu} U_{\mathbf{n}+\mu,\nu} U_{\mathbf{n}+\mu+\nu,\rho} \cdots), \quad (7)$$

where C is a closed path on the lattice and the right hand side is the trace of the product of the link variables along C . Note that the loop C can be larger than the lattice; one can just write a closed loop on the infinite lattice and impose the periodic boundary condition. This theory has the $(\mathbb{Z}_{N_c})^4$ center symmetry, which multiply a phase factor to the link variables:

$$U_{\mathbf{n},\mu} \rightarrow e^{2\pi i k_\mu / N_c} U_{\mathbf{n},\mu} \quad (k_\mu \in \mathbb{Z}). \quad (8)$$

Let us consider the 't Hooft large- N_c limit, in which the coupling constant b and the lattice size L are fixed. As long as the $(\mathbb{Z}_{N_c})^4$ center symmetry is not broken spontaneously, the expectation values of the Wilson loops do not depend on L . This is called the Eguchi-Kawai equivalence [3]. One can also introduce fermions with the periodic boundary condition; for example, for both the fundamental and adjoint fermions, the Dirac spectrum does not depend on L when N_f and the mass are fixed. Therefore one can study the large- N_c theory on the infinite lattice by using a small lattice, say 1^4 or 2^4 .

In the pure glue theory, the $(\mathbb{Z}_{N_c})^4$ center symmetry is actually broken in the weak coupling limit $b \rightarrow \infty$ with fixed L [16]. The breakdown of the center symmetry can easily be understood by calculating the one-loop effective action as a function of the Wilson line phases, by assuming four Wilson line phases to be static and diagonal. Then the off-diagonal fluctuation of the link variables provides an attractive interaction between the diagonal elements, so that the eigenvalues of the link variables favor the same value and hence the center symmetry breaks. It is nothing but the deconfinement transition in a very small volume.

Introducing the adjoint matter

The situation changes drastically when one adds the adjoint fermions, because they provide the repulsive force between eigenvalues. When one massless Majorana adjoint fermion is introduced, the theory is roughly the dimensional reduction of the four-dimensional $\mathcal{N} = 1$ pure super Yang-Mills theory. In the continuum theory, the forces acting on the Wilson line phases cancel to all

order in perturbation theory. By taking into account the nonperturbative effects, both the center-symmetric [17] and center-broken [18] phases can exist. (The importance of the nonperturbative effect was nicely demonstrated in a related context in [19].) Whether the center symmetry breaks or not on a lattice is a subtle issue which depends on the detail of the lattice regularization. If we add more massless adjoint fermions, the center symmetry is unbroken irrespectively of the detail of the lattice action [17]. Furthermore, somehow surprisingly at first glance, the center symmetry does not break spontaneously even with very heavy adjoint fermions, whose mass is as heavy as the ultraviolet cutoff scale [7, 20]; therefore one can study the pure Yang-Mills theory by using the EK equivalence⁷.

2.1.2 The orbifold equivalence

Another large- N_c equivalence, which turned out to be deeply related to the EK equivalence, was discovered by Lovelace [4]. He considered the $SO(2N_c)$, $USp(2N_c)$ and $SU(N_c)$ Yang-Mills theories and found that the Wilson loops take the same expectation values in all three theories. This equivalence was rediscovered and generalized in the study of the string theory [5], and a deeper understanding in terms of the field theory was obtained [29, 30]. Today it is called the orbifold equivalence.

The general statement is as follows. Let us start with the ‘parent’ theory, which is $SO(2N_c)$ or $USp(2N_c)$ in the case of [4]. We identify a discrete symmetry of the parent theory, which is a \mathbb{Z}_2 subgroup of the gauge symmetry in this example. Then we perform the ‘orbifold projection’ by keeping only the degrees of freedom which are invariant under the discrete symmetry, so that the ‘daughter’ theory ($SU(N_c)$) is obtained. If the projection satisfies a certain condition, the correlation functions of the operators in the parent theory which are invariant under the projection symmetry (the \mathbb{Z}_2 subgroup) and the correlation functions of the corresponding operators in the daughter theory take the same values, up to a calculable combinatoric factor. In particular, the expectation values of the chiral condensate take the same value in the $SO(2N_c)$, $USp(2N_c)$ and $SU(N_c)$ theories with the fundamental fermions. The EK equivalence can also be understood as a special example of the orbifold equivalence [17]. Other valuable applications include the large- N_c QCD at finite density [8, 31, 32, 33], confinement in pure Yang-Mills theory [34, 35], and interesting properties of non-supersymmetric daughters from supersymmetric parents [36, 37, 38].

3 The chiral random matrix theory (χ RMT)

In this section we provide a brief review of the χ RMT. For more details, see e.g. [39, 40].

We consider the ϵ -regime of QCD, where the space-time volume $V = L^4$ is taken such that L is much smaller than the pion Compton wavelength and is much larger than $1/\Lambda_{QCD}$ [41],

$$\frac{1}{\Lambda_{QCD}} \ll L \ll \frac{1}{m_\pi}. \quad (9)$$

In the ϵ -regime, the only relevant degrees of freedom are zero momentum modes of pions. Then the system has a *universality*, that is, the dynamics is determined by the symmetry breaking pattern

⁷ Another way to avoid the center symmetry breakdown is the double trace deformation [21, 22]. Other variants, quenched [16] and twisted [23] EK models, turned out to fail actually [24][25, 26, 27]. For a further modification of the twisted EK model may preserve the center symmetry, see [28].

and the microscopic details of the theory do not matter. Therefore QCD can be replaced by the χ RMT, which is a random matrix model with the same symmetry breaking pattern; in particular, the spectrum of the Dirac operator can be calculated from the χ RMT. Note that the same argument holds for other QCD-like theories as long as chiral symmetry is broken spontaneously.

The partition function of the χ RMT is given by

$$Z = \int d\Phi \prod_{f=1}^{N_f} \det \mathcal{D}_f e^{-\frac{N\beta}{2} G^2 \text{tr} \Phi^\dagger \Phi}, \quad (10)$$

where Φ is a $N \times (N + \nu)$ matrix and G is a normalization parameter. N corresponds to the size of the system (roughly speaking the space-time volume), and ν is the topological charge. Correspondingly to the thermodynamic limit of QCD, N is sent to infinity. In this limit, however, the fermion mass m_f must be scaled so that $m_f N$, which is (roughly speaking) identified with $m_f V$, is fixed.

Note that we can define the 't Hooft large- N limit (not the large- N_c limit) for the χ RMT, in which m_f is fixed. The limit one has to take for the comparison to QCD ($m_f N$ fixed) is *not* this 't Hooft limit. This difference is crucial when we compare the large- N_c gauge theories and χ RMT, as we will see in Sec. 4. In addition, it is important to notice that N is identified by the total degrees of freedom associated with the low-energy dynamics and the individual degrees of freedom, such as the volume and the number of colors, does not appear in the χ RMT explicitly.

The ensemble and the Dirac operator \mathcal{D} are chosen so that the Dirac operator has the same symmetries as the counterparts in QCD and QCD-like theories. Depending on the universality classes, there are three χ RMTs, which are distinguished by the Dyson index $\beta = 1$, $\beta = 2$, and $\beta = 4$ [42]:

- $\beta = 2$ (e.g. QCD and $SU(N_c)$ ($N_c \geq 3$) with the fundamental fermions):

$$\mathcal{D}_f = \begin{pmatrix} m_f \mathbf{1} & \Phi \\ -\Phi^\dagger & m_f \mathbf{1} \end{pmatrix}, \quad (11)$$

where Φ is an $N \times (N + \nu)$ complex matrix and m_f ($f = 1, 2, \dots, N_f$) are the fermion masses.

- $\beta = 1$ (e.g. $SU(2)$ and $USp(2N_c)$ with the fundamental fermions):

$$\mathcal{D}_f = \begin{pmatrix} m_f \mathbf{1} & \Phi \\ -\Phi^T & m_f \mathbf{1} \end{pmatrix}, \quad (12)$$

where Φ is an $N \times (N + \nu)$ real matrix.

- $\beta = 4$ (e.g. $SU(N_c)$ with the adjoint fermions and $SO(2N_c)$ with the fundamental fermions):

$$\mathcal{D}_f = \begin{pmatrix} m_f \mathbf{1} & \Phi \\ -\Phi^\dagger & m_f \mathbf{1} \end{pmatrix}, \quad (13)$$

where Φ is a $2N \times 2(N + \nu)$ quaternion real matrix, which can be written by using four $N \times (N + \nu)$ real matrices ϕ_0, ϕ_1, ϕ_2 and ϕ_3 as

$$\Phi = \begin{pmatrix} \phi_0 + i\phi_3 & i\phi_1 + \phi_2 \\ i\phi_1 - \phi_2 & \phi_0 - i\phi_3 \end{pmatrix}. \quad (14)$$

Because of its simplicity, the χ RMT can be solved analytically. It has been applied not just to the test of $S\chi$ SB in the lattice simulations, but also to other important problems such as the QCD at a finite baryon chemical potential [43, 44] and the phase structure of the Wilson Dirac operator [45, 46, 47].

4 Large- N_c versus χ RMT

In this section, we establish the way to use the χ RMT techniques in large- N_c gauge theories. For concreteness, we consider the $SU(N_c)$ lattice theory with volume V and fermion mass m . Here the volume V is arbitrary, although we concentrate on a small fixed volume in Sec. 5.

4.1 Difference of the limits

In order to compare the large- N_c gauge theory and χ RMT, we must understand the difference of the limits, which are required for the standard $1/N_c$ -counting and the universality, respectively:

- When one compares the χ RMT with the gauge theory, the matrix size N of the χ RMT is identified with the degrees of freedom in the gauge theory which are important for the low-energy dynamics, $N \sim VN_c^\alpha$, where the constant α depends on the representation of the fermion in general. (As we will see, $\alpha = 1$ for the massless probe adjoint fermion of the 2^4 -lattice model. Note that it is different from the usual counting in the 't Hooft limit, $\alpha = 2$.) In order for the universality to hold, $mN \sim mVN_c^\alpha$ must be fixed as we take the large- N_c limit. Let us call it the ' χ RMT limit'. This limit is compatible with the condition for the ε regime in Eq. 9.
- For the standard $1/N_c$ counting, the ordinary 't Hooft large- N_c limit, in which m and V are fixed, must be taken. In this limit the large- N_c equivalences (e.g. the EK equivalence) hold.

The χ RMT limit is different from the 't Hooft limit and the standard 't Hooft $1/N_c$ -counting does not hold in this limit. In order to see this, let us consider the k -point connected correlation function in the χ RMT (see e.g. [42])

$$\langle (\bar{\psi}\psi)^k/N \rangle_{conn,RMT} = \left\langle \frac{1}{N} \sum_{i=1}^{2N} \left(\frac{1}{\lambda_i + m} \right)^k \right\rangle_{RMT}, \quad (15)$$

where λ_i are eigenvalues of the Dirac operator. In the 't Hooft counting, $\langle (\bar{\psi}\psi)^k/N \rangle_{conn,RMT}$ is of order N^0 . It is true when m is of order one: $1/(\lambda_i + m)^k$ is of order one and the summation over $2N$ order-one quantities is of order N . However when m scales as $1/N$, the smallest of $\lambda_i + m$ is also of order $1/N$, and hence the correlation function becomes of order N^{k-1} . This divergence is analogous to the infrared divergence in $SU(3)$ QCD in the ε -regime. (Note that $\bar{\psi}\psi$ in χ RMT corresponds to $\int d^4x \bar{\psi}\psi$ in QCD.) In large- N_c field theories, this corresponds to the divergence with a certain power of N_c , which is different from the 't Hooft counting. This peculiar behavior can also be understood in terms of the large- N_c gauge theory; because the coefficients $c_{g,b}$ in (4) are functions of m and V , they can have nontrivial N_c -dependences in the χ RMT limit, where m and V are scaled with N_c .

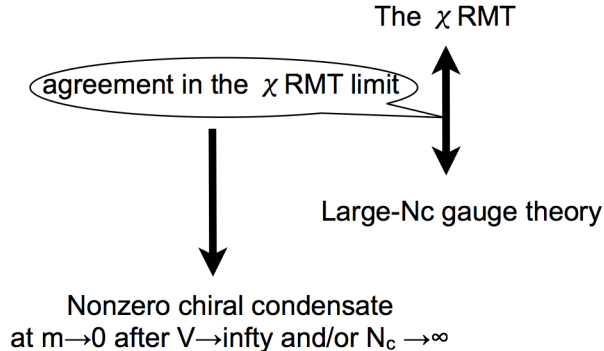


Figure 2: The agreement between the χ RMT and the large- N_c gauge theory in the χ RMT limit assures $S\chi$ SB in the 't Hooft limit and/or the large-volume limit.

Because of this difference, the large- N_c equivalences do not hold in the χ RMT limit. As an example, let us consider the chiral condensate in $SU(N_c)$, $SO(2N_c)$ and $USp(2N_c)$ theories. In the planar limit, because of the orbifold equivalence (Sec. 2.1.2), they are the same as a function of m [8, 31]. On the other hand, in the χ RMT limit they can be calculated by using the χ RMTs as a function of mN , and they do behave differently [48, 49]. It means the orbifold equivalence does not hold there. (Note that it is the case even in the quenched theory, which we numerically study in this paper.)

4.2 The comparison

First let us recall how one can realize $S\chi$ SB in numerical simulations of QCD in the ε -regime. The criterion for $S\chi$ SB is whether the Dirac spectrum agrees with the χ RMT prediction. Once they are found to agree, the value of the chiral condensate is determined. Notice that the value of the chiral condensate obtained in the ε -regime is the same as the one obtained by taking the chiral limit after the large-volume (or thermodynamic) limit. It means that, whatever the order of the limiting procedures is, we can determine the chiral condensate.

The same logic should hold for large N_c gauge theories. But this time, the role of the volume in the χ RMT limit can be played by N_c . Namely, the χ RMT limit is achieved by taking the large N_c limit with mVN_c^α fixed. Then, the criterion for $S\chi$ SB is again the agreement of the Dirac spectrum in the χ RMT (Fig. 2).

In Fig. 3 we show how one can combine the χ RMT and the EK equivalence to see $S\chi$ SB. We compare the spectrum of the Dirac operator of the probe fermion with the mass $m \sim N_c^{-\alpha}$ in the $V = 2^4$ lattice and that in the χ RMT; the agreement between them implies the breakdown of chiral symmetry (nonzero chiral condensate) in the 't Hooft limit. Using the EK equivalence, therefore, we conclude that chiral symmetry is spontaneously broken in the large-volume lattice gauge theories. The constant α is determined by the *effective* degrees of freedom in the low mode region. As we will see, in the 2^4 -lattice model with the massless probe adjoint fermion, small eigenvalues scales as $1/N_c$. Therefore we take $\alpha = 1$ ⁸. We also found a nice agreement of the

⁸ In [14] the same scaling has been already found for the $N_f = 1$ theory with a very small mass (which is

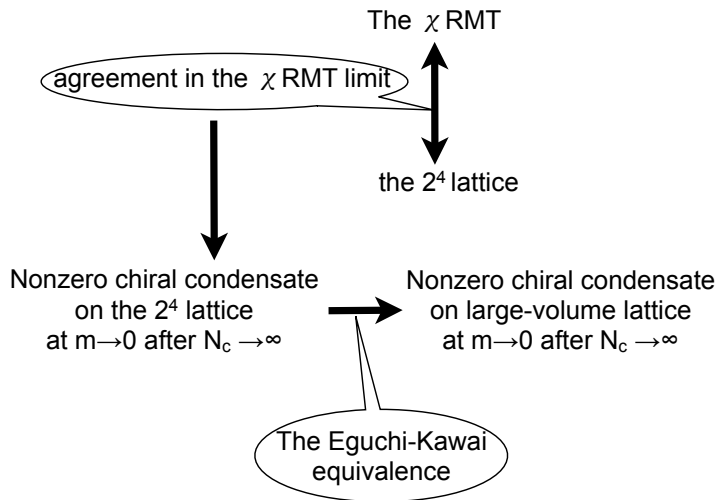


Figure 3: The agreement between the χ RMT and the 2^4 -lattice model in the χ RMT limit implies $S\chi$ SB or equivalently non-zero chiral condensate in the 't Hooft limit. Then, one can use the EK equivalence to conclude $S\chi$ SB in the large-volume theory.

low-lying Dirac spectrum, which we interpret as the presence of $S\chi$ SB.

Here let us discuss the N_c scaling of the chiral condensate for later use. In the large-volume theory, the chiral condensate Σ of the adjoint fermion is related with the spectral density $\rho(\lambda)$ by the Banks-Casher relation [50],

$$\Sigma = |\langle \bar{\psi}\psi \rangle| = \pi\rho(0), \quad \text{with} \quad \rho(\lambda) = \left\langle \frac{1}{V} \sum_n \delta(\lambda - \lambda_n) \right\rangle, \quad (16)$$

where λ_n is the Dirac eigenvalues. The spectral density at $\lambda = 0$ is proportional to the inverse of spacing of the near-zero Dirac eigenvalues, $\Delta\lambda = \lambda_{i+1} - \lambda_i$. $\Delta\lambda$ is expected to scale like $\sim 1/N$, where N is the number of degrees of freedom important for the low-energy dynamics. Since the definition of $\rho(\lambda)$ in (16) is already normalized by V , ρ thus defined scales as N_c increases. In the 't Hooft limit, the degrees of freedom of both gauge and fermion parts are $O(N_c^2)$ and as a consequence $\Sigma = N_c^2 \tilde{\Sigma}$ in the 't Hooft limit, where an $O(N^0)$ quantity $\tilde{\Sigma}$ is defined by the *properly normalized operator* as

$$\tilde{\Sigma} = \frac{1}{N_c^2} |\langle \text{tr}(\bar{\psi}\psi) \rangle| = \pi\tilde{\rho}(0), \quad \text{with} \quad \tilde{\rho}(\lambda) = \left\langle \frac{1}{VN_c^2} \sum_n \delta(\lambda - \lambda_n) \right\rangle. \quad (17)$$

In the χ RMT limit, however, we have to carefully count the number of degrees of freedom associated with the low-energy dynamics which may be different from that in the 't Hooft limit; in general the properly normalized spectral density would be related with the spacing of small Dirac

essentially massless). In that paper, however, the authors regard that the deviation from the 't Hooft counting $\alpha = 2$ suggests the absence of $S\chi$ SB.

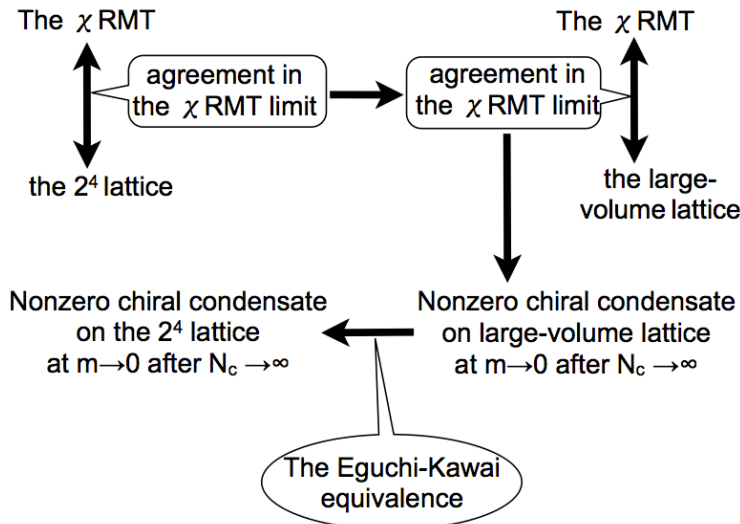


Figure 4: Another interpretation. The agreement between the χ RMT and the 2^4 -lattice model in the χ RMT limit translates into the agreement the χ RMT and the large-volume lattice thanks to the absence of the phase transition (the center symmetry breakdown). One can conclude S χ SB of the large-volume theory from the agreement between χ RMT and the 2^4 -lattice model in the χ RMT limit.

eigenvalues by $\tilde{\rho}(0) = 1/(VN^\alpha\Delta\lambda)$, where the α mentioned above is determined from how the low-lying eigenvalues scale with N_c .

Strictly speaking, there is a subtlety in the χ RMT limit of the 2^4 -lattice model: because the space-time volume of this lattice is very small, usual derivation of the χ RMT from QCD via the chiral perturbation theory may not be applicable⁹. In order to circumvent this subtlety, one can take another path (Fig. 4) as follows. First let us consider a sufficiently large volume, where the usual derivation of the χ RMT is valid when chiral symmetry is spontaneously broken. Then, the distribution of the Dirac eigenvalues should agree with that from the χ RMT after properly normalizing the eigenvalues by $\lambda(VN^\alpha)\tilde{\Sigma}$. Therefore, as long as V is large enough to justify the chiral perturbation, V -dependence does not appear manifestly. Now let us shrink the volume further. If we consider the pure Yang-Mills without the (heavy) adjoint fermion, there is a phase transition (the breakdown of the center symmetry), beyond which one cannot expect the same expression for the distribution of the Dirac eigenvalues. However in the present case, because there is no phase transition thanks to the heavy adjoint fermion, it is expected that the same expression for the eigenvalue distribution holds at very small volume as a function of $\lambda(VN_c^\alpha)\tilde{\Sigma}$, where the value of α could be different from that in the large-volume theory. (In order to confirm this argument a quantitative study of $\tilde{\Sigma}$ on a large lattice is required and therefore we leave it as our future work.) Then, the agreement between the χ RMT and the 2^4 -lattice model in the RMT limit translates into the agreement between the χ RMT and the large-volume lattice provided

⁹ One might think the standard mapping rule between the planar sector of the small-volume (i.e. EK model) and the large-volume theory can be used. However nonplanar diagrams can contribute in the χ RMT limit.

unbroken center symmetry. At large volume and in the 't Hooft limit, one can conclude S χ SB in the ordinary manner. By further using the EK equivalence, S χ SB of the 2⁴-lattice model in the 't Hooft limit can also be concluded.

5 Numerical simulation of the 2⁴-lattice model and comparison to χ RMT

In this section, we apply the strategy explained in Sec. 4 to the 2⁴-lattice model and detect S χ SB. After introducing the lattice action and simulation details in Sec. 5.1, in Sec. 5.2 we confirm that the center symmetry, which is crucial for the use of the EK equivalence, can be kept unbroken by adding heavy adjoint fermions. Then, in Sec. 5.3 we calculate the Dirac spectrum and compare with the χ RMT prediction.

For an earlier work along the same direction, see [13]. See also [51, 52] for recent numerical simulations of a single-site model.

5.1 Lattice action and simulation details

We take the standard the Wilson plaquette gauge action Eq. 5,

$$S_g = 2N_c^2 b \sum_{\mathbf{n}} \sum_{\mu < \nu} \left(1 - \frac{1}{N_c} \text{ReTr} P_{\mu\nu}(\mathbf{n}) \right), \quad \mathbf{n} \in 2^4. \quad (18)$$

In order to preserve the center symmetry, we add two-flavor of heavy adjoint fermions, for which we choose the plain Wilson fermion,

$$S_f = \sum_{j=1}^2 \sum_{\mathbf{n}} \bar{\psi}_{\mathbf{n},j} \left(\psi_{\mathbf{n},j} - \kappa \sum_{\mu}^4 \left[(1 - \gamma_{\mu}) U_{\mathbf{n},\mu}^{adj} \psi_{\mathbf{n}+\mu,j} + (1 + \gamma_{\mu}) U_{\mathbf{n}-\mu,\mu}^{\dagger,adj} \psi_{\mathbf{n}-\mu,j} \right] \right), \quad (19)$$

where b and κ represent the inverse of the 't Hooft coupling, $b = 1/(g_{YM}^2 N_c)$, and the hopping parameter, $\kappa = (2m_0 a + 8)^{-1}$ (where m_0 is the bare fermion mass), respectively. The plaquette $P_{\mu\nu}$ is defined by Eq. 6. For the fermionic action, the link variables in the adjoint representation are defined by

$$U_{a,b}^{adj} = \frac{1}{2} \text{Tr}[T_F^a U T_F^b U^{\dagger}], \quad (20)$$

where T_F^a are $SU(N_c)$ generators in the fundamental representation. This action is invariant under $SU(N_c)$ local gauge transformation

$$U_{\mathbf{n},\mu} \longrightarrow \Omega_{\mathbf{n}} U_{\mathbf{n},\mu} \Omega_{\mathbf{n}+\mu}^{\dagger}, \quad \Omega_{\mathbf{n}} \in SU(N_c), \quad (21)$$

as well as $(\mathbb{Z}_{N_c})^4$ global center transformation Eq. 8. Throughout this work, we impose periodic boundary conditions in all directions for both link variables and fermion fields.

Our lattice simulations consist of two parts: 1) quenched calculations ($\kappa = 0$), where $m_0 a$ is infinite, as a nontrivial check of our numerical code by confirming the breaking of center symmetry at weak coupling, 2) simulations with two heavy adjoint fermions ($\kappa = 0.09$), where the center

Table 1: Simulation parameters.

κ	b	N_c	N_{conf}	κ	b	N_c	N_{conf}
0	0.3	8	500	0.09	0.2	6	465
		8	500			8	458
	0.5	2	200		0.5	2	150
		3	200			3	150
		4	600			4	150
		5	500			5	500
		6	200			6	500
		8	500			8	500
		10	500			10	300
		11	300			11	400
		15	200			12	250
16	400	15	138				
				16	500		

symmetry is unbroken even at weak coupling while the low-energy dynamics are essentially the same as those of pure $SU(N_c)$ gauge theory since m_0 is of order of the inverse lattice spacing.

Simulation parameters are summarized in Table 1. We performed simulations at $b = 0.5$ (weak coupling) for up to $N_c = 16$, which is relatively smaller than that in previous single-site model simulations [7, 20, 51]. As we will see in Sec. 5.2.2, however, we could obtain good large- N_c limits since we have additional suppression of the finite volume effects thanks to the larger volume of a 2^4 lattice. For $N_c = 8$ and $\kappa = 0$, we also performed simulations at $b = 0.3$ and 0.4 corresponding to the strong and intermediate couplings, respectively. In addition, we performed simulations at $b = 0.2$ (strong coupling) for $\kappa = 0.09$ and $N_c = 6, 8$. We used the Hybrid Monte Carlo (HMC) algorithm for all lattice simulations with the plain leap-frog integrator, where the step size is tuned such that the acceptance ratio is in the range of 70 – 80 %. The simulation codes were developed from the one used in [53] with appropriate modification to $SU(N_c)$ adjoint fermions with arbitrary large N_c . After 200 trajectories for thermalization, $N_{conf} = 138 - 600$ configurations are accumulated for each ensemble, where every two adjacent configurations are separated by 10 trajectories. Statistical errors are calculated by using the standard bootstrapping technique.

5.2 $(\mathbb{Z}_{N_c})^4$ Center Symmetry

As explained in Sec. 2.1.1, the non-trivial condition for the large- N_c EK equivalence is that the $(\mathbb{Z}_{N_c})^4$ center symmetry of the reduced volume theory must be unbroken. The presence of the center symmetry is established by checking the followings: (1) the Polyakov loop radially scatters in the vicinity of origin in the complex plane, (2) the magnitude of the Polyakov loop approaches zero as N_c increases, (3) the average plaquette value measured in the reduced model agrees with that in the large-volume lattice gauge theory. In this section, we present our findings for pure $SU(N_c)$ gauge theory and the theory with two heavy adjoint fermions.

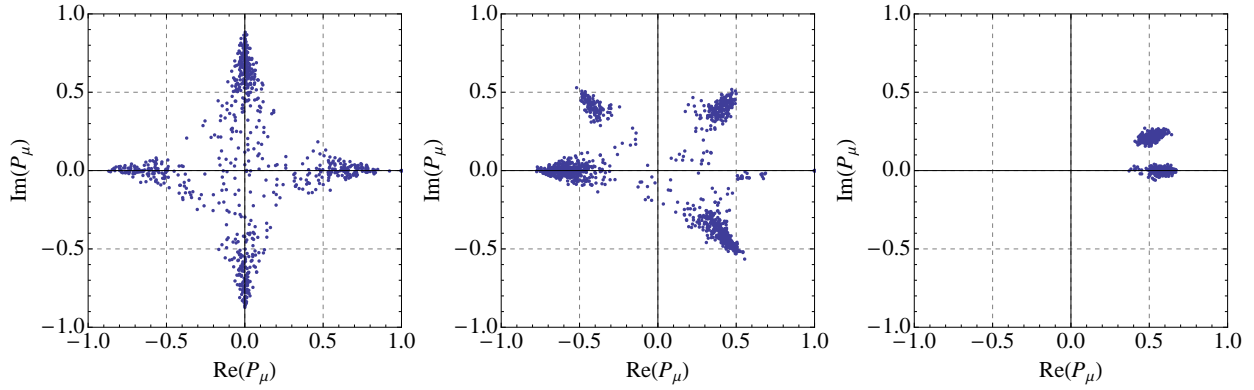


Figure 5: Scatter plots of the Polyakov loops for quenched simulations with $b = 0.5$. The number of colors are $N_c = 4, 8$, and 16 from the left to right.

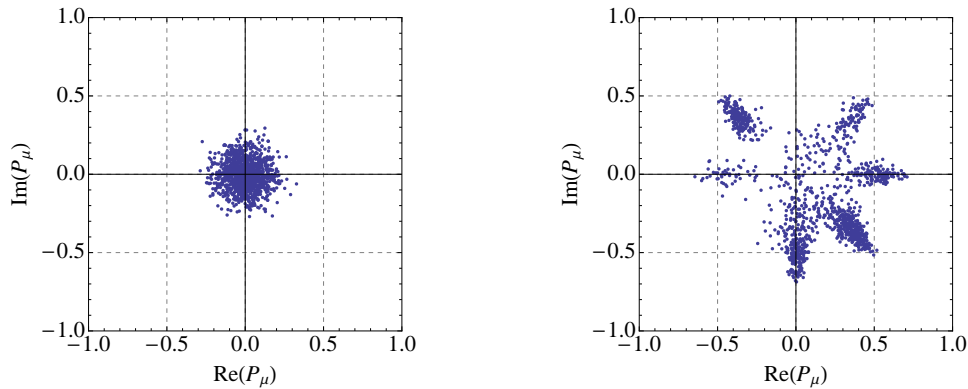


Figure 6: Scatter plots of the Polyakov loops for quenched simulations with $N_c = 8$. The values of the couplings are $b = 0.3$ and 0.4 from left to right.

5.2.1 Pure $SU(N_c)$ gauge theory

In Fig. 5, we show scatter plots¹⁰ of the Polyakov loops defined by

$$P_{\mu=1}(y, z, w) = \frac{1}{N_c} \text{Tr} U_{\mu=1;0,y,z,w} U_{\mu=1;1,y,z,w}, \quad (22)$$

and similarly for $\mu = 2, 3$ and 4 , where $b = 0.5$ and $N_c = 4, 8, 16$ from left to right. In this weak coupling regime, the plots clearly show the center symmetry breaking as the Polyakov loops are localized at the elements of the center of $SU(N_c)$, $2in_\mu\pi/N_c$, where $n_\mu = 0, 1, \dots, N_c - 1$. For a given number of configurations, the number of clusters decreases to one as the number of colors N_c increases from 5 to 16 ; this means the tunneling transitions between different center-symmetry-broken vacua will eventually disappear at $N_c \rightarrow \infty$.

For $N_c = 8$, we performed two more simulations with smaller values of b . The results of the Polyakov loops are shown in Fig. 6. At $b = 0.3$, the Polyakov loops develop a cluster around the

¹⁰For all scatter plots, We used about a hundred ensembles and chose one of the direction μ out of four directions. We found similar scatter plots for three other directions.

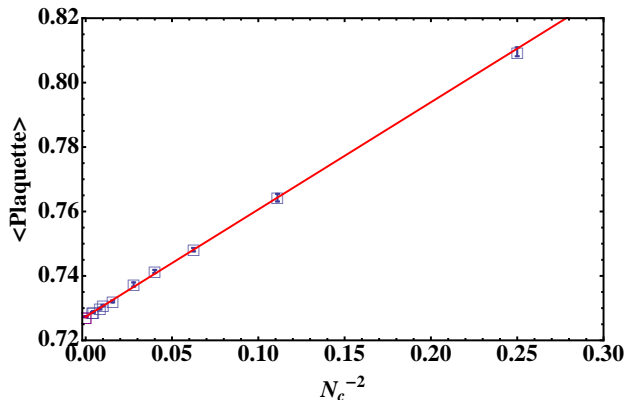


Figure 7: Average plaquette values for quenched simulations with $b = 0.5$. The red solid line represents the uncorrelated fit of the data to the function, $c_0 + c_1/N_c^2$, and we obtained $c_0 = 0.72733(12)$ and $c_1 = 0.3325(46)$, where the chi-square/d.o.f is 0.67.

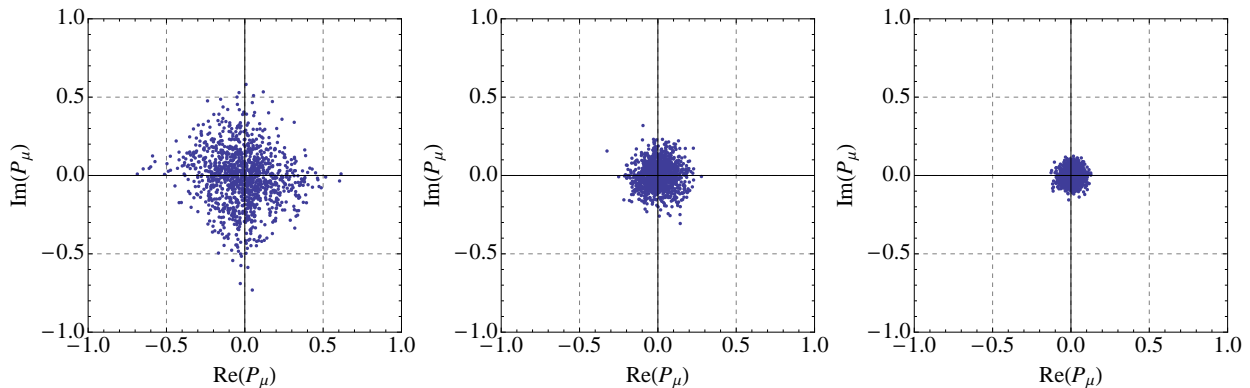


Figure 8: Scatter plots of the Polyakov loops at $b = 0.5$ with two heavy adjoint fermions. The number of colors are $N_c = 4, 8, 16$ from left to right.

origin, while at $b = 0.4$ they spread out and are localized at the center-symmetry-broken vacua like at $b = 0.5$. Therefore, we conclude that the center symmetry is restored in the strong coupling regime. The boundary between the strong and weak coupling regimes is located somewhere between $b = 0.3$ and $b = 0.4$, which is consistent with the results in [54].

In Fig. 7, we plotted average plaquette values for N_c up to 16. The measured plaquette values turn out to scale as $1/N_c^2$ and thus we perform a fit to the data using a constant plus quadratic function of N_c^{-1} (red solid line in the figure). We obtained $0.72733(12)$ in the large N_c limit, which is larger than 0.7182 , the value from large-volume lattice gauge theory [7]. Therefore we reproduced the well-known fact that the large- N_c volume reduction for pure Yang-Mills theory fails at weak coupling due to absence of the center symmetry.

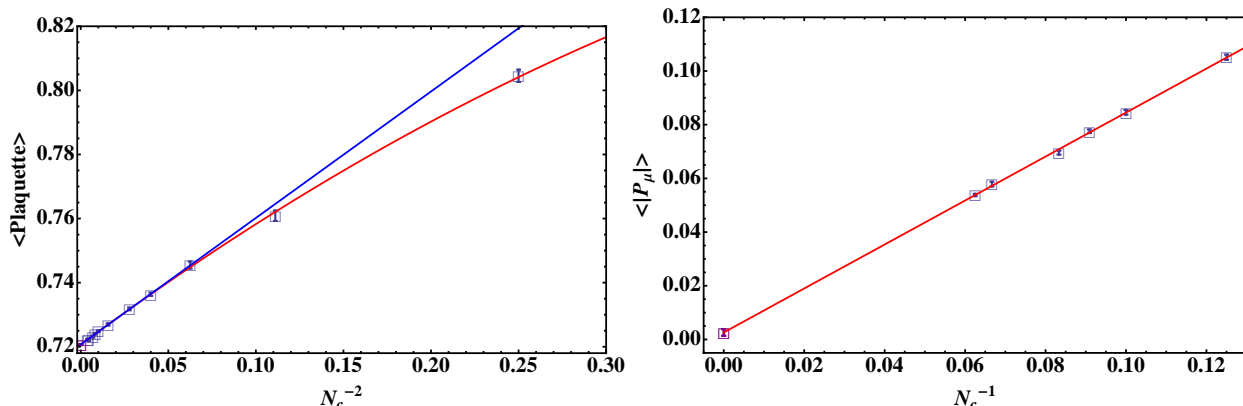


Figure 9: (Left) Average plaquette values and (Right) average values of the magnitudes of the Polyakov loops along with fit results in Table 2.

Table 2: Fit results for the Polyakov loop and plaquette values.

	Data set	Fit function	c_0	c_1	c_2	$\chi^2/\text{d.o.f}$
Plaquette	$N_c = [4, 16]$	$c_0 + c_1/N_c + c_2/N_c^2$	0.72053(71)	0.003(13)	0.383(50)	0.47
	$N_c = [2, 16]$	$c_0 + c_1/N_c^2 + c_2/N_c^4$	0.72067(14)	0.405(12)	-0.283(61)	0.49
Polyakov loop	$N_c = [5, 16]$	$c_0 + c_1/N_c$	0.0026(12)	0.819(15)		0.89

5.2.2 $SU(N_c)$ gauge theory with two heavy adjoint fermions

Now let us add two heavy adjoint fermions in order to keep the center symmetry unbroken even at weak coupling. At $b = 0.5$, we performed a set of simulations for various values of N_c with fixed value of $\kappa = 0.09$ as shown in Table 1. In Fig. 8, we show scatter plots of the Polyakov loops for $N_c = 4, 8$, and 16. The clustering of the Polyakov loops around the origin for $N_c = 8$ and 16 clearly shows that the center symmetry is intact, which is in contrast to the case without adjoint fermions.

In Fig. 9, we show the average plaquette values versus N_c^{-2} and the magnitudes of the Polyakov loops versus N_c^{-1} . For the plaquette values, we examined two different fits, one fitting the data of $4 \leq N_c \leq 16$ to $c_0 + c_1/N_c + c_2/N_c^2$ (blue solid line) and the other fitting those of $2 \leq N_c \leq 16$ to $c_0 + c_1/N_c^2 + c_2/N_c^4$ (red solid line). For the Polyakov loops, we fit the data of $5 \leq N_c \leq 16$ to $c_0 + c_1/N_c$ to obtain the large N_c limit. The fit results are summarized in Table 2.

As discussed in [20] and [51] in great details, the leading correction to plaquette in the large- N_c limit for a single-site lattice model is $O(1/N_c)$, instead of $O(1/N_c^2)$ (in the usual 't Hooft counting), due to the contributions of diagonal zero modes. If we apply this argument to our non-single site reduced model, the $1/N_c$ correction term is suppressed by $1/V$. Indeed, we obtained a consistent result where the one-sixteenth of the coefficient of $1/N_c$ calculated in [20]¹¹ is within the uncertainty of our results shown in Table 2 (first row). The extracted plaquette value also agrees with that obtained in a single-site model [20], but it is systematically larger than that from the large-volume lattice calculation for pure Yang-Mills. This tiny difference comes from the presence of heavy fermions. The magnitude of the Polyakov loop goes to zero as N_c increases;

¹¹The value of the coefficient is 0.22 ± 0.01 , which was not presented in the original paper.

it scales as $1/N_c$ in the asymptotic region. Therefore, we conclude that the center symmetry is unbroken for a given lattice parameters and thus the EK volume equivalence is applicable.

5.3 Comparison to χ RMT

As discussed in Sec. 4, to detect $S\chi$ SB we compare the low-lying Dirac eigenmodes of the 2^4 -lattice model with those of χ RMT in the limit of $N_c \rightarrow \infty$ with mVN_c^α fixed. The simplest way to achieve the χ RMT limit without losing the generality might be taking $m = 0$ and $N_c \rightarrow \infty$ ¹². For this purpose, we calculate the low-lying spectrum of the overlap-Dirac operator \mathcal{D} for a massless fermion in the adjoint representation. The operator \mathcal{D} is defined by

$$\mathcal{D} = M \left[1 + \gamma_5 \frac{H_w(-M)}{\sqrt{H_w(-M)H_w(-M)^\dagger}} \right], \quad (23)$$

where $H_w(-M)$ is the hermitian Wilson-Dirac operator and the parameter M is taken to be 1.6 in the most cases. The overlap-Dirac eigenvalues $\tilde{\lambda}_k$ lie on a circle in the complex plane [55, 56]. To compare the Dirac spectrum with the χ RMT, we consider the projection of the eigenvalues to the imaginary axis,

$$\lambda_k = \frac{\text{Im}[\tilde{\lambda}_k]}{1 - \text{Re}[\tilde{\lambda}_k]/m_0}. \quad (24)$$

Note that the Dirac eigenvalues for adjoint fermions are appearing as conjugate pairs with 2-fold degeneracy and we take the distinct eigenvalues on the upper-half plane for our numerical results. Unless otherwise noted, the numerical results in this section are restricted to the case of $b = 0.5$ (weak coupling).

5.3.1 Chiral symmetry breaking

As seen in Sec. 5.2, the adjoint fermion plays a role of the center symmetry preserver in the 2^4 -lattice model. Since the EK volume equivalence is valid for the same lattice parameters such as the bare coupling and the fermion mass, the equivalent large-volume theory also has the fermion mass of order $O(1/a)$ and approximates the quenched theory. As a comparison, therefore, we consider the χ RMT for the quenched theory. We restrict the χ RMT predictions to the case of zero-topological charge. Accordingly, the configurations yielding exact zero mode(s) are omitted from the analysis.

The adjoint QCD with any number of flavors belongs to the universal class of the Chiral Gaussian Symplectic Ensemble (ChGSE). However, we also consider two other universal classes, Chiral Gaussian Orthogonal Ensemble (ChGOE) and Chiral Gaussian Unitary Ensemble (ChGUE), in order to make the comparison manifest. The distributions of the lowest eigenvalue are

$$P(z) = \begin{cases} \frac{2+z}{4} e^{-(z/2)-(z^2/8)} & \text{for ChGOE} \\ \frac{z}{2} e^{-z^2/4} & \text{for ChGUE} , \\ \sqrt{\frac{\pi}{2}} z^{(3/2)} I_{3/2}(z) e^{-z^2/2} & \text{for ChGSE} \end{cases} \quad (25)$$

¹²Although this limit looks like the 't Hooft limit (m is fixed), actually one should not regard it so because the infrared (IR) regulator is assumed in the usual 't Hooft counting; for the usual 't Hooft counting one must introduce nonzero fixed m as an IR regulator and takes the large- N_c limit, and then sends the mass to zero.

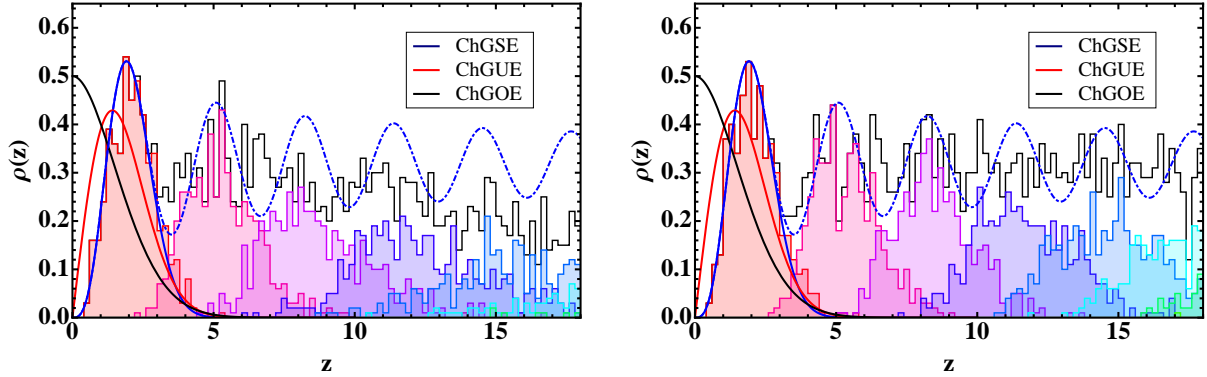


Figure 10: Low-lying Dirac spectrum for $N_c = 8$ (left) and $N_c = 16$ (right). The Dirac eigenvalues are rescaled by matching the ensemble average of the lowest eigenvalue with the expectation value of the lowest eigenvalue in the χ RMT for the ChGSE. The solid and dotted lines represent the χ RMT predictions of the distributions of the lowest eigenvalue and the spectral density, respectively. The colored histograms are for individual eigenvalues, while the black histograms are for all eigenvalues.

and the spectral densities [49] are

$$\rho(z) = \begin{cases} \frac{z}{2} [J_0^2(z) + J_1^2(z)] + \frac{1}{2} J_0(z) [1 - \int_0^z dt J_0(t)] & \text{for ChGOE} \\ \frac{z}{2} [J_0^2(z) + J_1^2(z)] & \text{for ChGUE} \\ z [J_0^2(2z) + J_1^2(2z)] - \frac{1}{2} J_0(2z) \int_0^{2z} dt J_0(t) & \text{for ChGSE} \end{cases} \quad (26)$$

Histograms of the lowest twelve Dirac eigenvalues for $N_c = 8, 16$ at $b = 0.5$ and $\kappa = 0.09$ are shown in Fig. 10. For the lowest eigenvalue, we found that its distribution is well described by the χ RMT for the ChGSE (solid blue curve) after introducing a rescaled eigenvalue z by $z = \lambda V \Sigma$ to fit the data, where $V = 2^4$ and Σ is a free parameter. As a comparison, we show the distribution of the lowest eigenvalue predicted by the χ RMT for the ChGUE (solid red curve) and ChGOE (solid black curve) using the same parameter z for the ChGSE. In addition, we plot the spectral densities for the ChGSE (dashed blue curve), which are in good agreement with a few lowest eigenvalues. According to Fig. 3, this result would be a strong evidence that chiral symmetry of quenched large N_c gauge theory is spontaneously broken.

In Fig. 11, we compare $\delta\langle\lambda_k\rangle/\langle\lambda_1\rangle$ for $N_c = 16$ (our largest value of N_c) with the χ RMT prediction, where the bracket $\langle\cdots\rangle$ represents the ensemble average. The low-lying Dirac eigenvalues perfectly agree with the χ RMT prediction, which adds a further evidence for $S\chi$ SB. We have also studied the strong coupling region, $b = 0.2$, and similarly found a good agreement with the χ RMT prediction (see Fig. 15). However, note that this point is actually stronger coupling than the bulk phase transition; this phase is not related to the continuum limit a priori.

5.3.2 N_c -scaling and gap of the Dirac eigenvalues

In Sec. 4, we argued that the χ RMT limit of the 2^4 -lattice model is analogous to that of ordinary QCD by replacing mV with $mV N_c^\alpha$, where the exponent α can be determined so that N_c^α is the number of degrees of freedom important at low energy, which is proportional to the inverse of the

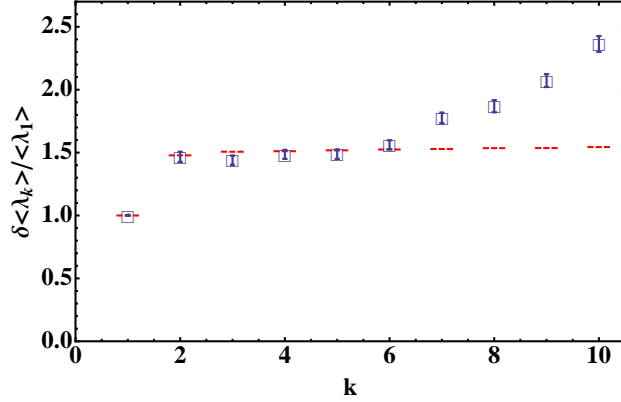


Figure 11: Spacing between the adjacent Dirac eigenvalues normalized by the lowest eigenvalue $\langle \lambda_1 \rangle$ for $N_c = 16$, where $\delta \langle \lambda_k \rangle = \langle \lambda_k \rangle - \langle \lambda_{k-1} \rangle$ and $\langle \lambda_0 \rangle = 0$. The red dashed lines represent the χ RMT prediction for the $\beta = 4$ universal class.

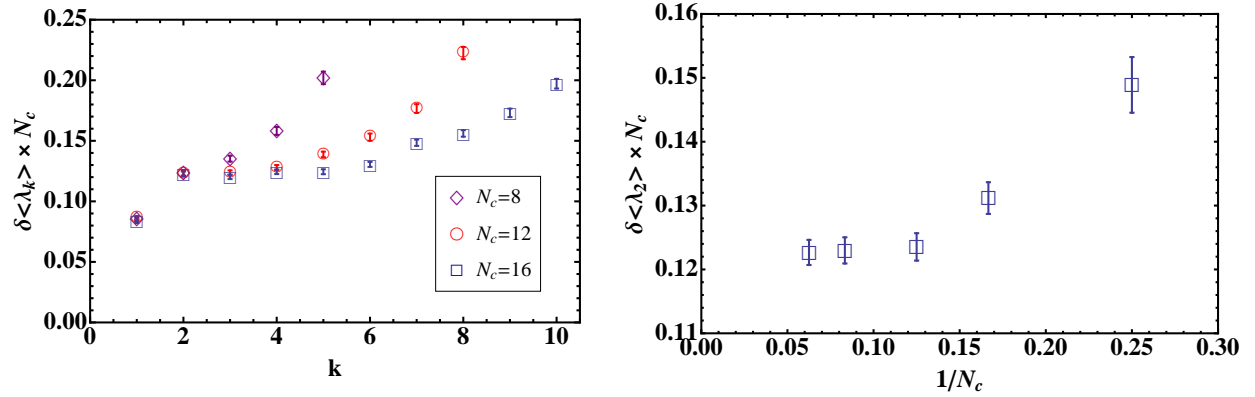


Figure 12: (Left) Spacing between the adjacent Dirac eigenvalues multiplied by N_c for $N_c = 8, 12$ and 16 . (Right) Spacing between the first and second Dirac eigenvalues multiplied by N_c for $N_c = 4, 6, 8, 12$ and 16 .

eigenvalue density around the origin. Then, because the low-lying eigenvalues scale as $1/N_c$ as we will see below, we obtain $\alpha = 1$.

In the left panel of Fig. 12, we plot the spacing between the adjacent low-lying Dirac eigenvalues multiplied by N_c for $N_c = 8, 12$ and 16 . We see a nice agreement of the data points at up to $k = 2$ for $N_c = 8$ and at up to $k = 4$ for $N_c = 12$, where the spacings are expected to show a plateau for $k \geq 2$. This result implies that the near-zero eigenvalues, which are expected to reproduce the χ RMT prediction well, scale as $1/N_c$. (The same scaling had been reported in [14], by using the single-site model with a very light dynamical overlap adjoint fermion.) The right figure of Fig. 12 shows $\delta \langle \lambda_2 \rangle$ multiplied by N_c for various N_c ; for given statistics, they agree to each other for $N_c \geq 8$. We find that the eigenvalue spacing deviates from the χ RMT prediction as we increase k or decrease N_c ; the distribution has a long-tail in the direction of the large eigenvalue. This behavior can be understood as follows. As we will see below, the *gap* appears between the $(N_c - 1)$ -

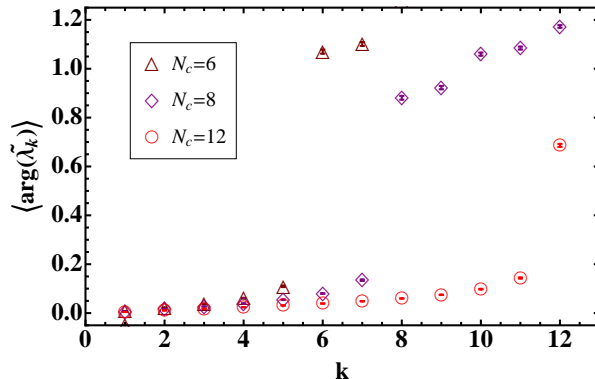


Figure 13: Low-lying overlap-Dirac eigenvalues in units of radian for $N_c = 6, 8, 12$.

th and N_c -th eigenvalues, where the spectral density is zero. The repulsion between eigenvalues becomes weaker as we approach the *gap*, and thus the distribution develops a long-tail to the *gap*. Therefore, the eigenvalue spacing near the gap becomes larger than expected. Note also that the $1/N_c$ correction takes a rather complicated form due to the peculiar distribution; for $\delta\lambda_2$, though at $N_c = 4, 6, 8$ the correction looks $1/N_c$, at $N_c \geq 8$ this behavior disappears and the value stays almost constant. For $\delta\lambda_3$ we observe a similar $1/N_c$ -like behavior at $N_c = 8, 12$ and 16, but we expect the value is saturated at $N_c \simeq 16$.

To describe this *gap* clearly, we plot the lowest twelve overlap-Dirac eigenvalues, which lie on a circle in the complex plane, in units of radian for $N_c = 6, 8$ and 12 in Fig. 13. The eigenvalue abruptly jumps at $k = 5, 7$ and 11 for $N_c = 6, 8$ and 12, respectively. (A similar *gap* had also been found in the $N_f = 1$ theory [14].) For $k < N_c$, the eigenvalue spacing roughly scales as $1/N_c$ or equivalently the density scales as N_c . The gap persists in the large- N_c limit: the N_c -th eigenvalues are reasonably well fit by the function $0.3 + 4.6N_c^{-1}$. The schematic diagram of the overlap-Dirac eigenvalues on a circle in the complex plane is shown in Fig. 14. The N_c -dependence of the eigenvalue density is expected to change from N_c to N_c^2 as k changes from $k < N_c$ to $k \geq N_c$.

A possible explanation of the $1/N_c$ -scaling of Dirac eigenvalues and the appearance of a *gap* relies on the perturbative analysis around the diagonal Wilson lines for a weakly coupled gauge fields. In the perturbation theory, the spectrum of the theory is governed by the background of the Wilson lines and thus the low-lying Dirac spectrum should be closely related to the zero modes [20]. For the fermions in the adjoint representation the number of zero modes of the Wilson lines is $(N_c - 1)$, which is the *effective* number of degrees of freedom, while the number of total degrees of freedom is N_c^2 . According to our argument in Sec. 4, therefore, the low-lying Dirac eigenvalues should scale as $1/N_c$, being consistent with our numerical results. We emphasize that this analysis is only true for weakly coupled large N gauge theory in a *compact space*.

When $N_f = 1$, the position of this *gap* has been studied for several values of the coupling constant [14], which turned out to be almost independent of the coupling constant in the lattice unit. Therefore, in the physical unit, the scale corresponding to the location of the gap diverges as the lattice cutoff increases. This result looks natural, because a new physical scale appears otherwise.

It is also satisfactory from the universality point of view: $SU(N_c)$ theory with N_f adjoint

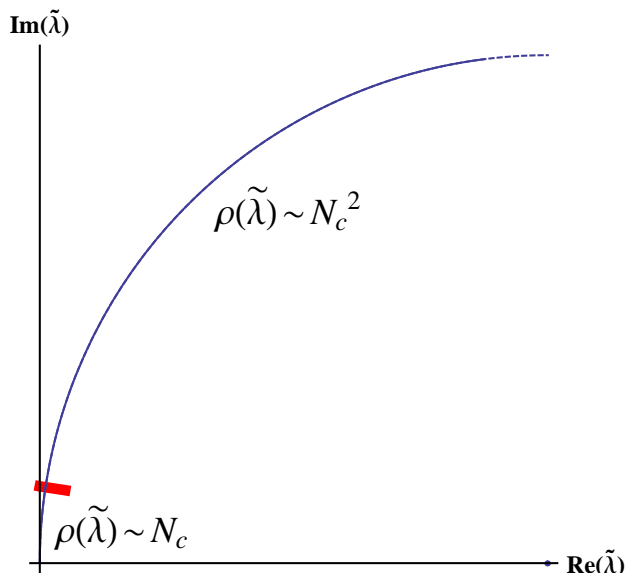


Figure 14: (Right) Schematic diagram of the eigenvalue density of the overlap-Dirac operator on a circle in the complex plane.

fermions and $SO(2N_c)$ theory with N_f fundamental fermions are equivalent in the χ RMT limit, because they are described by the same χ RMT. However they are completely different in the 't Hooft large- N_c limit; whereas the former has $O(N_c^2)$ fermion degrees of freedom, the latter has only $O(N_c)$. In order for them to become identical in the χ RMT limit, the fermionic degrees of freedom must match somehow. But now we know the mechanism: only $O(N_c)$ degrees of freedom survives in the low energy limit of the adjoint theory, because $N_c^2 - N_c$ eigenvalues become infinitely large. (In the case of the fundamental fermions in the probe limit, there is no *gap* [6]).

At strong coupling phase, the perturbative treatment around the diagonal background Wilson lines is no longer reliable: the zero modes can be lifted by gauge fluctuation and the off-diagonal components would be the same order of magnitude of the diagonal components. In contrast to the case of weak coupling, therefore, we expect that the *gap* is absent and the eigenvalue spacing is of order $O(1/N_c^2)$. In the left panel of Fig. 15, we plot the eigenvalue spacing multiplied by N_c^2 for $N_c = 6$ (red circle) and $N_c = 8$ (blue square) and at $b = 0.2$. The data shows a nice plateau and agrees to each other, implying that the eigenvalue scales as $1/N_c^2$ without any *gap* in the strong coupling regime, as expected. In the same manner, it is expected that the Dirac eigenvalues scale as $1/N_c^2$ and the gap does not exist even at weak coupling if the volume is sufficiently large: as the volume increases the momentum gap between the lowest and the first excited state, which differ by $(2\pi/L)$, decreases and at some point the zero modes are lifted by gauge fluctuation.

6 Conclusion and discussion

In this paper we considered how to apply the χ RMT techniques to large- N_c gauge theories. After giving general considerations, we provided a numerical demonstration by using the 2^4 -lattice model as an example. The most important lesson is that the 't Hooft large- N_c limit and the χ RMT limit

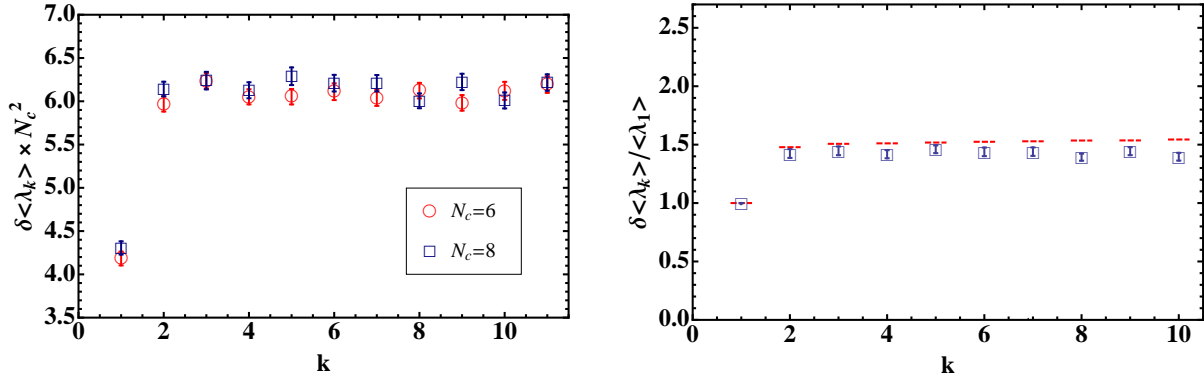


Figure 15: (Left) Spacing of the adjacent Dirac eigenvalues multiplied by N_c^2 for $N_c = 6, 8$ with $b = 0.2$, where $\delta\langle\lambda_k\rangle = \langle\lambda_k\rangle - \langle\lambda_{k-1}\rangle$ and $\langle\lambda_0\rangle = 0$. (Right) Spacing between the adjacent Dirac eigenvalues normalized by the lowest eigenvalue $\langle\lambda_1\rangle$. The red dashed lines represent the χ RMT prediction for the $\beta = 4$ universal class.

(the microscopic limit) are not compatible in general: the former is the large- N_c limit with the fermion mass m and the space-time volume V fixed, while the latter requires mVN_c^α to be fixed, where α is a positive constant which may depend on the theory. The value of α is a unity in the example we studied in Sec. 5, which is different from the usual 't Hooft counting.

An important consequence of the difference between two limits is that several properties in the 't Hooft large- N_c limit (e.g. the equivalence between $SU(N_c)$, $SO(2N_c)$ and $USp(2N_c)$ gauge theories) do not hold in the χ RMT limit. This fact must be appreciated when one applies the large- N_c and/or χ RMT approaches to QCD and related theories; although these two approaches provide valuable 'exact' results, they are valid in different parameter regions and hence one has to carefully choose more suitable method depending on the physics he/she studies. In spite of the difference of two limits, one can still detect $S\chi$ SB of large- N_c gauge theories as we have demonstrated in Sec. 5.

Rather curiously, we observed a nice agreement between the χ RMT and 2^4 -lattice model even when the center symmetry in the latter is broken spontaneously. Of course we cannot relate this fact to $S\chi$ SB in the large-volume theory, because neither the EK equivalence nor the analytic continuation can be used. This is presumably because the space-time dimension is not important for the universality argument; only the pattern of $S\chi$ SB matters.

As a next step, we are studying whether the $SU(N_c)$ gauge theory with dynamical adjoint fermions goes through $S\chi$ SB or not, with an application to technicolor models in mind. We hope to report the result in near future.

Acknowledgements

The authors would like to thank S. Hashimoto, A. Hietanen, M. Kieburg, M. Koren, S. Sharpe, M. Tezuka, J. Verbaarschot and N. Yamamoto for stimulating discussions and comments. The numerical computations used in this work were carried out on cluster at KEK. M. H. would like to thank Boston University for hospitality at the final stage of this work. This work is supported in part by the Grant-in-Aid for Scientific Research of the Japanese Ministry of Education, Culture,

Sports, Science and Technology and JSPS (Nos. 20105002,20105005,and 22740183).

References

- [1] H. Fukaya *et al.*, “Two-flavor lattice QCD simulation in the epsilon-regime with exact chiral symmetry,” *Phys.Rev.Lett.*, vol. 98, p. 172001, 2007.
- [2] G. 't Hooft, “A Planar Diagram Theory for Strong Interactions,” *Nucl.Phys.*, vol. B72, p. 461, 1974.
- [3] T. Eguchi and H. Kawai, “Reduction of Dynamical Degrees of Freedom in the Large N Gauge Theory,” *Phys. Rev. Lett.*, vol. 48, p. 1063, 1982.
- [4] C. Lovelace, “UNIVERSALITY AT LARGE N,” *Nucl.Phys.*, vol. B201, p. 333, 1982.
- [5] S. Kachru and E. Silverstein, “4-D conformal theories and strings on orbifolds,” *Phys.Rev.Lett.*, vol. 80, pp. 4855–4858, 1998.
- [6] R. Narayanan and H. Neuberger, “Chiral symmetry breaking at large N(c),” *Nucl. Phys.*, vol. B696, pp. 107–140, 2004.
- [7] B. Bringoltz and S. R. Sharpe, “Non-perturbative volume-reduction of large-N QCD with adjoint fermions,” *Phys. Rev.*, vol. D80, p. 065031, 2009.
- [8] A. Cherman, M. Hanada, and D. Robles-Llana, “Orbifold equivalence and the sign problem at finite baryon density,” *Phys. Rev. Lett.*, vol. 106, p. 091603, 2011.
- [9] F. Sannino and K. Tuominen, “Orientifold theory dynamics and symmetry breaking,” *Phys.Rev.*, vol. D71, p. 051901, 2005.
- [10] M. A. Luty and T. Okui, “Conformal technicolor,” *JHEP*, vol. 0609, p. 070, 2006.
- [11] L. Del Debbio, “The conformal window on the lattice,” *PoS*, vol. LATTICE2010, p. 004, 2010.
- [12] D. D. Dietrich and F. Sannino, “Conformal window of SU(N) gauge theories with fermions in higher dimensional representations,” *Phys.Rev.*, vol. D75, p. 085018, 2007.
- [13] A. Hietanen and R. Narayanan, “The large N limit of four dimensional Yang-Mills field coupled to adjoint fermions on a single site lattice,” *JHEP*, vol. 01, p. 079, 2010.
- [14] A. Hietanen and R. Narayanan, “Numerical evidence for non-analytic behavior in the beta function of large N SU(N) gauge theory coupled to an adjoint Dirac fermion,” *Phys.Rev.*, vol. D86, p. 085002, 2012.
- [15] J. M. Maldacena, “The Large N limit of superconformal field theories and supergravity,” *Adv.Theor.Math.Phys.*, vol. 2, pp. 231–252, 1998.
- [16] G. Bhanot, U. M. Heller, and H. Neuberger, “The Quenched Eguchi-Kawai Model,” *Phys. Lett.*, vol. B113, p. 47, 1982.

- [17] P. Kovtun, M. Unsal, and L. G. Yaffe, “Volume independence in large $N(c)$ QCD-like gauge theories,” *JHEP*, vol. 06, p. 019, 2007.
- [18] M. Hanada and I. Kanamori, “Lattice study of two-dimensional $N=(2,2)$ super Yang-Mills at large- N ,” *Phys.Rev.*, vol. D80, p. 065014, 2009.
- [19] H. Aoki, S. Iso, H. Kawai, Y. Kitazawa, and T. Tada, “Space-time structures from IIB matrix model,” *Prog.Theor.Phys.*, vol. 99, pp. 713–746, 1998.
- [20] T. Azeyanagi, M. Hanada, M. Unsal, and R. Yacoby, “Large- N reduction in QCD-like theories with massive adjoint fermions,” *Phys. Rev.*, vol. D82, p. 125013, 2010.
- [21] M. Unsal and L. G. Yaffe, “Center-stabilized Yang-Mills theory: Confinement and large N volume independence,” *Phys.Rev.*, vol. D78, p. 065035, 2008.
- [22] H. Vairinhos, “Phase transitions in center-stabilized lattice gauge theories,” *PoS*, vol. LATTICE2011, p. 252, 2011.
- [23] A. Gonzalez-Arroyo and M. Okawa, “The Twisted Eguchi-Kawai Model: A Reduced Model for Large N Lattice Gauge Theory,” *Phys. Rev.*, vol. D27, p. 2397, 1983.
- [24] B. Bringoltz and S. R. Sharpe, “Breakdown of large- N quenched reduction in $SU(N)$ lattice gauge theories,” *Phys. Rev.*, vol. D78, p. 034507, 2008.
- [25] W. Bietenholz, J. Nishimura, Y. Susaki, and J. Volkholz, “A non-perturbative study of 4d $U(1)$ non-commutative gauge theory: The fate of one-loop instability,” *JHEP*, vol. 10, p. 042, 2006.
- [26] T. Azeyanagi, M. Hanada, T. Hirata, and T. Ishikawa, “Phase structure of twisted Eguchi-Kawai model,” *JHEP*, vol. 01, p. 025, 2008.
- [27] M. Teper and H. Vairinhos, “Symmetry breaking In twisted Eguchi-Kawai models,” *Phys. Lett.*, vol. B652, pp. 359–369, 2007.
- [28] A. Gonzalez-Arroyo and M. Okawa, “Large N reduction with the Twisted Eguchi-Kawai model,” *JHEP*, vol. 07, p. 043, 2010.
- [29] M. Bershadsky and A. Johansen, “Large N limit of orbifold field theories,” *Nucl.Phys.*, vol. B536, pp. 141–148, 1998.
- [30] P. Kovtun, M. Unsal, and L. G. Yaffe, “Necessary and sufficient conditions for non-perturbative equivalences of large $N(c)$ orbifold gauge theories,” *JHEP*, vol. 0507, p. 008, 2005.
- [31] M. Hanada and N. Yamamoto, “Universality of Phases in QCD and QCD-like Theories,” *JHEP*, vol. 02, p. 138, 2012.
- [32] A. Cherman and B. C. Tiburzi, “Orbifold equivalence for finite density QCD and effective field theory,” *JHEP*, vol. 1106, p. 034, 2011.

- [33] Y. Hidaka and N. Yamamoto, “No-Go Theorem for Critical Phenomena in Large- N_c QCD,” *Phys.Rev.Lett.*, vol. 108, p. 121601, 2012.
- [34] M. Unsal, “Abelian duality, confinement, and chiral symmetry breaking in QCD(adj),” *Phys.Rev.Lett.*, vol. 100, p. 032005, 2008.
- [35] M. Shifman and M. Unsal, “QCD-like Theories on $R(3) \times S(1)$: A Smooth Journey from Small to Large $r(S(1))$ with Double-Trace Deformations,” *Phys.Rev.*, vol. D78, p. 065004, 2008.
- [36] M. Schmaltz, “Duality of nonsupersymmetric large N gauge theories,” *Phys.Rev.*, vol. D59, p. 105018, 1999.
- [37] M. J. Strassler, “On methods for extracting exact nonperturbative results in nonsupersymmetric gauge theories,” 2001.
- [38] A. Armoni, M. Shifman, and G. Veneziano, “Exact results in nonsupersymmetric large N orientifold field theories,” *Nucl.Phys.*, vol. B667, pp. 170–182, 2003.
- [39] J. Verbaarschot and T. Wettig, “Random matrix theory and chiral symmetry in QCD,” *Ann.Rev.Nucl.Part.Sci.*, vol. 50, pp. 343–410, 2000.
- [40] G. Akemann, “Matrix Models and QCD with Chemical Potential,” *Int.J.Mod.Phys.*, vol. A22, pp. 1077–1122, 2007.
- [41] H. Leutwyler and A. V. Smilga, “Spectrum of Dirac operator and role of winding number in QCD,” *Phys.Rev.*, vol. D46, pp. 5607–5632, 1992.
- [42] J. J. M. Verbaarschot, “The Spectrum of the QCD Dirac operator and chiral random matrix theory: The Threefold way,” *Phys.Rev.Lett.*, vol. 72, pp. 2531–2533, 1994.
- [43] M. A. Stephanov, “Random matrix model of QCD at finite density and the nature of the quenched limit,” *Phys.Rev.Lett.*, vol. 76, pp. 4472–4475, 1996.
- [44] J. Osborn, K. Splittorff, and J. Verbaarschot, “Chiral symmetry breaking and the Dirac spectrum at nonzero chemical potential,” *Phys.Rev.Lett.*, vol. 94, p. 202001, 2005.
- [45] G. Akemann, P. Damgaard, K. Splittorff, and J. Verbaarschot, “Spectrum of the Wilson Dirac Operator at Finite Lattice Spacings,” *Phys.Rev.*, vol. D83, p. 085014, 2011.
- [46] K. Splittorff, “Chiral Dynamics With Wilson Fermions,” 2012.
- [47] G. Akemann and F. Pucci, “Exploring the Aoki regime,” 2012.
- [48] J. Verbaarschot, “Universal scaling of the valence quark mass dependence of the chiral condensate,” *Phys.Lett.*, vol. B368, pp. 137–142, 1996.
- [49] D. Toublan and J. Verbaarschot, “The Spectral density of the QCD Dirac operator and patterns of chiral symmetry breaking,” *Nucl.Phys.*, vol. B560, pp. 259–282, 1999.

- [50] T. Banks and A. Casher, “Chiral Symmetry Breaking in Confining Theories,” *Nucl.Phys.*, vol. B169, p. 103, 1980.
- [51] B. Bringoltz, M. Koren, and S. R. Sharpe, “Large-N reduction in QCD with two adjoint Dirac fermions,” *Phys.Rev.*, vol. D85, p. 094504, 2012.
- [52] A. Gonzalez-Arroyo and M. Okawa, “Twisted reduction in large N QCD with two adjoint Wilson fermions,” 2012.
- [53] S. Aoki *et al.*, “Two-flavor QCD simulation with exact chiral symmetry,” *Phys.Rev.*, vol. D78, p. 014508, 2008.
- [54] S. Catterall, R. Galvez, and M. Unsal, “Realization of Center Symmetry in Two Adjoint Flavor Large-N Yang-Mills,” *JHEP*, vol. 08, p. 010, 2010.
- [55] H. Neuberger, “Exactly massless quarks on the lattice,” *Phys.Lett.*, vol. B417, pp. 141–144, 1998.
- [56] H. Neuberger, “More about exactly massless quarks on the lattice,” *Phys.Lett.*, vol. B427, pp. 353–355, 1998.